

Quo Vadis Flavour Anomalies?

Marcin Chrząszcz
mchrzasz@cern.ch



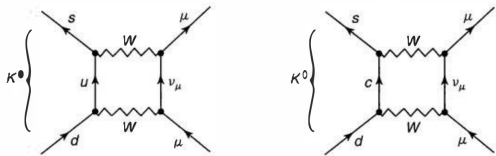
Białasówka seminar
November 30, 2018

Outline

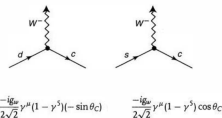
1. Why flavour is important.
2. The flavour anomalies:
 - $R(D^*)$
 - R_K and R_{K^*}
 - P'_5
3. Global fits results.
4. Robustness of SM prediction.
5. Conclusions.

Why Flavour is important?

A lesson from history - GIM mechanism



- Cabibbo angle was successful in explaining dozens of decay rates in the 1960s.
- There was, however, one that was not observed by experiments: $K^0 \rightarrow \mu^- \mu^+$.
- Glashow, Iliopoulos, Maiani (GIM) mechanism was proposed in the 1970 to fix this problem. The mechanism required the existence of a 4th quark.
- At that point most of the people were skeptical about that. Fortunately in 1974 the discovery of the J/ψ meson silenced the skeptics.



$$\frac{-ig_W}{2\sqrt{2}} \gamma^\mu (1 - \gamma^5) (-\sin \theta_C)$$

$$\frac{-ig_W}{2\sqrt{2}} \gamma^\mu (1 - \gamma^5) \cos \theta_C$$

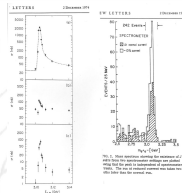
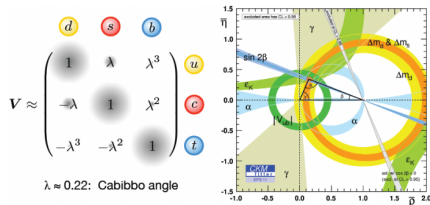
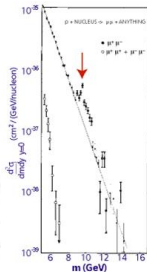


Fig. 1. Cross section versus energy for the decay $J/\psi \rightarrow e^+e^-$ and $J/\psi \rightarrow \mu^+\mu^-$. The solid line is the theoretical prediction for the decay into two leptons and the dashed line is the experimental data. The inset shows the decay $J/\psi \rightarrow \gamma\gamma$. The solid line is the theoretical prediction for the decay into two photons and the dashed line is the experimental data.

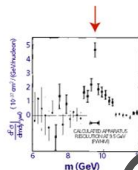
A lesson from history - CKM matrix



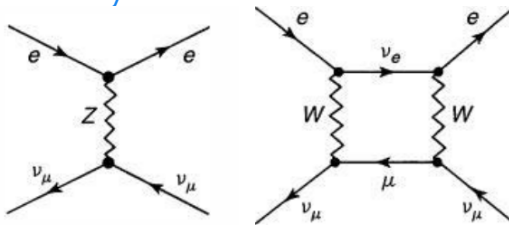
- Similarly, CP violation was discovered in 1960s in the neutral kaons decays.
- 2×2 Cabbibo matrix could not allow for any CP violation.
- For CP violation to be possible one needs at least a 3×3 unitary matrix \rightarrow Cabibbo-Kobayashi-Maskawa matrix (1973).
- It predicts existence of b (1977) and t (1995) quarks.



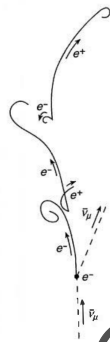
Results published in
Physical Review Letters
August 1, 1977



A lesson from history - Weak neutral current



- Weak neutral currents were first introduced in 1958 by Buldman.
- Later on they were naturally incorporated into unification of weak and electromagnetic interactions.
- 't Hooft proved that the GWS models was renormalizable.
- Everything was there on theory side, only missing piece was the experiment, till 1973.



Study the CKM matrix

Arises from Higgs Yukawa interactions
Unitary in the SM, with one CP violating phase.

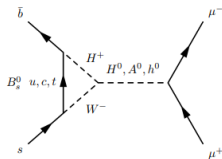
$$\begin{pmatrix} d' \\ s' \\ b' \end{pmatrix} = \begin{pmatrix} V_{ud} & V_{us} & V_{ub} \\ V_{cd} & V_{cs} & V_{cb} \\ V_{td} & V_{ts} & V_{tb} \end{pmatrix} \begin{pmatrix} d \\ s \\ b \end{pmatrix} = V_{CKM} \begin{pmatrix} d \\ s \\ b \end{pmatrix}$$

Test unitarity with many measurements.

Find new sources of CPV
wru anti-matter!?

Measure decays of ground state b-hadrons

Properties influenced by virtual particles in NP models
Compare results to SM predictions
(need QCD input).



Particularly sensitive to NP models preferring third generation.

Study the CKM matrix

Arises from Higgs Yukawa interactions

Unitary in the SM, with one CP violating phase.

$$\begin{pmatrix} d' \\ s' \\ b' \end{pmatrix} = \begin{pmatrix} V_{ud} & V_{us} & V_{ub} \\ V_{cd} & V_{cs} & V_{cb} \\ V_{td} & V_{ts} & V_{tb} \end{pmatrix} \begin{pmatrix} d \\ s \\ b \end{pmatrix} = V_{CKM} \begin{pmatrix} d \\ s \\ b \end{pmatrix}$$

Test unitarity with many measurements.

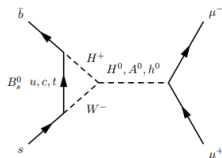
Find new sources of CPV
wru anti-matter!?

Measure decays of ground state b-hadrons

Properties influenced by virtual particles in NP models

Compare results to SM predictions

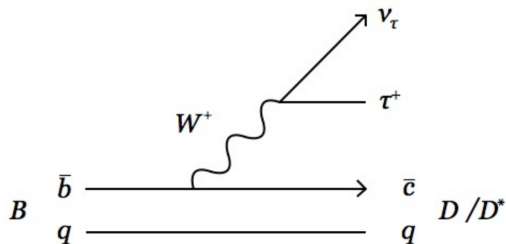
(need QCD input).



Particularly sensitive to NP models preferring third generation.

Why semi-leptonic decays?

⇒ A decay is semi-leptonic if its products are part leptons and part hadrons.



$$\frac{d\Gamma}{dq^2}(B \rightarrow D l \nu) \propto$$

$$G_F^2 |V_{cb}|^2 f(q^2)^2$$

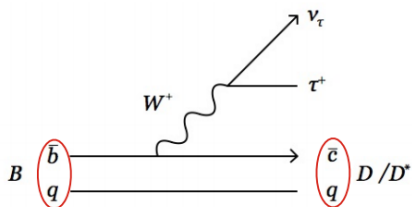
EW QCD

⇒ These decays can be factorised into the weak and strong parts, greatly simplifying theoretical calculations.

Types of semi-leptonic decays

Two types of semi-leptonic b-decay

Charged current

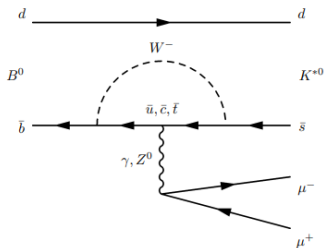


Can proceed via tree level - large $O(\%)$ branching fractions.

Factorised up to (small) QED corrections.

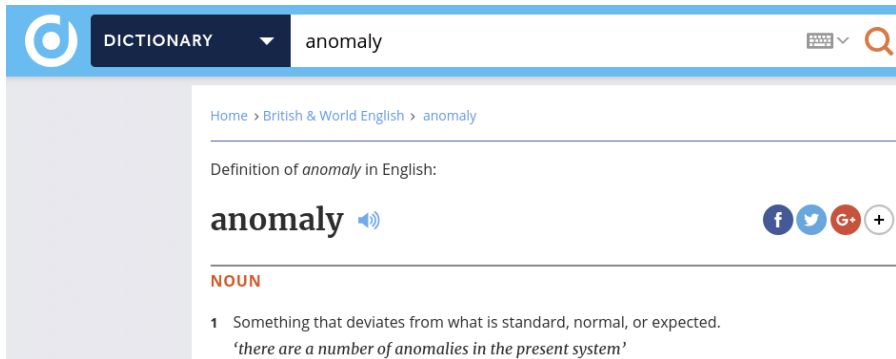
When you factorise, QCD part broken down into form-factors.

Neutral current



Forbidden at tree level - low $O(10^{-6})$ branching fractions.


Factorised up to corrections from $B \rightarrow h(\rightarrow \mu^+ \mu^-)h$ decays.







The screenshot shows the Cambridge Dictionary interface. At the top, there is a navigation bar with the Cambridge logo on the left, a dark blue button labeled 'DICTIONARY' with a dropdown arrow, and a search bar containing the word 'anomaly'. To the right of the search bar are icons for a keyboard and a magnifying glass. Below the navigation bar, the breadcrumb trail reads 'Home > British & World English > anomaly'. The main content area features the text 'Definition of *anomaly* in English:' followed by the word 'anomaly' in a large, bold font with a speaker icon for audio playback. To the right of the word are social media sharing icons for Facebook, Twitter, Google+, and a plus sign for more options. Below this, the word is categorized as 'NOUN' in orange. A numbered definition follows: '1 Something that deviates from what is standard, normal, or expected. *'there are a number of anomalies in the present system'*'.

Home > British & World English > anomaly

Definition of *anomaly* in English:

anomaly 

NOUN

1 Something that deviates from what is standard, normal, or expected.
'there are a number of anomalies in the present system'

⇒ Today I will talk about three anomalies in B decays:

- $R(D^*)$
- R_{K/K^*}
- P'_5

Anomaly 1

$$R(D^*) = \frac{\mathcal{B}(B \rightarrow D^* \tau \nu)}{\mathcal{B}(B \rightarrow D^* \mu \nu)}$$

$R(D^*)$

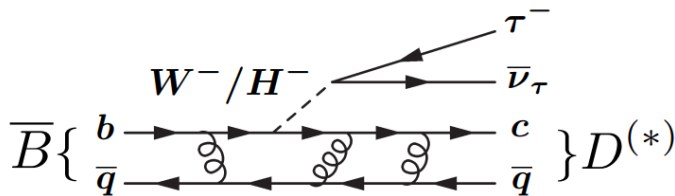
⇒ Large rate of charged current decays allow for measurement in semi-tauonic decays

$$R(D^*) = \frac{\mathcal{B}(B \rightarrow D^* \tau \nu)}{\mathcal{B}(B \rightarrow D^* \mu \nu)}$$

⇒ Form ratio of decays with different lepton generations.

⇒ Cancel QCD uncertainties.

⇒ $R(D^*)$ is sensitive to the NP with strong 3rd generation couplings.



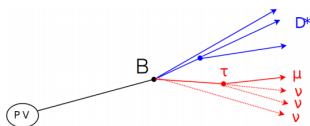
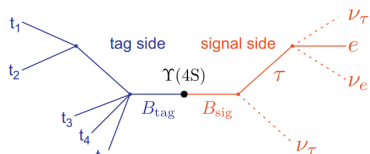
The Rule of three

	BaBar	Belle	LHCb
#B's produced	O(400M)	O(700M)	O(800B)*
Production mechanism	$\Upsilon(4S) \rightarrow B\bar{B}$	$\Upsilon(4S) \rightarrow B\bar{B}$	$pp \rightarrow gg \rightarrow b\bar{b}$
Publications	Phys.Rev.Lett 109, 101802 (2012) Phys. Rev. D 88, 072012 (2013)	Phys.Rev.D 92, 072014 (2015) arXiv:1603.06711	Phys.Rev.Lett. 115, 111803 (2015)

Experimental challenges

- ⇒ With the $\tau \rightarrow \mu\nu\nu$ decay we are missing 3 neutrinos!
- ⇒ No sharp peak in any distributions.

⇒ At B-factories, can control this using tagging technique.

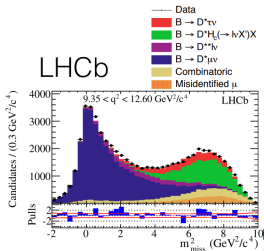
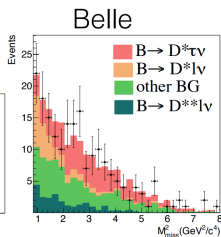
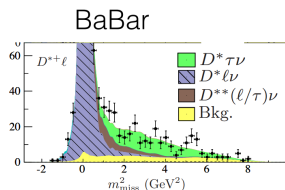


⇒ More difficult at LHCb, compensate using large boost (flight information) and huge B production

Signal fits

⇒ Three main backgrounds:

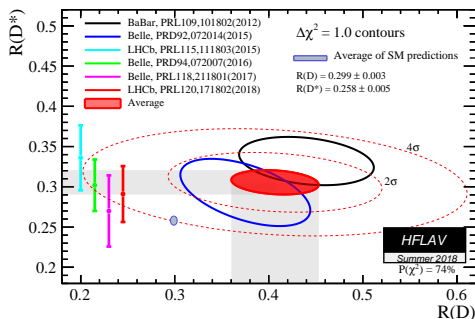
- $B \rightarrow D^* \ell \nu$.
- $B \rightarrow D^{**} \ell \nu$.
- $B \rightarrow DD^* X$



⇒ Fit variables which discriminate between the signal and background modes.

Results

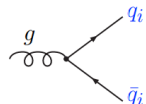
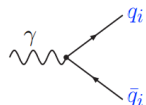
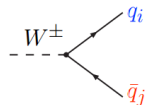
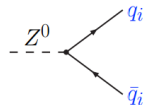
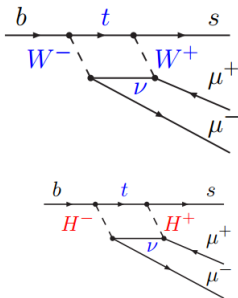
⇒ All experiments see an access w.r.t. to SM prediction:



- ⇒ Theoretical uncertainties negligible.
- ⇒ The ball is on the experimental side.

Introduction to anomaly 2 & 3

- The SM allows only the charged interactions to change flavour.
 - Other interactions are flavour conserving.
- One can escape this constraint and produce $b \rightarrow s$ and $b \rightarrow d$ at loop level.
 - These kind of processes are suppressed in SM \rightarrow Rare decays.
 - New Physics can enter in the loops.

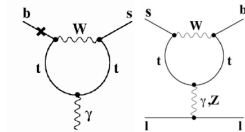


Analysis of Rare decays

Analysis of FCNC in a model-independent approach, effective Hamiltonian:

$$b \rightarrow s\gamma(^*) : \mathcal{H}_{\Delta F=1}^{SM} \propto \sum_{i=1}^{10} V_{ts}^* V_{tb} \mathcal{C}_i \mathcal{O}_i + \dots$$

- $\mathcal{O}_7 = \frac{e}{16\pi^2} m_b (\bar{s} \sigma^{\mu\nu} P_R b) F_{\mu\nu}$
- $\mathcal{O}_9 = \frac{e^2}{16\pi^2} (\bar{s} \gamma_\mu P_L b) (\bar{\ell} \gamma_\mu \ell)$
- $\mathcal{O}_{10} = \frac{e^2}{16\pi^2} (\bar{s} \gamma_\mu P_L b) (\bar{\ell} \gamma_\mu \gamma_5 \ell), \dots$



- **SM** Wilson coefficients up to NNLO + e.m. corrections at $\mu_{ref} = 4.8$ GeV [Misiak et al.]:

$$\mathcal{C}_7^{SM} = -0.29, \mathcal{C}_9^{SM} = 4.1, \mathcal{C}_{10}^{SM} = -4.3$$

- **NP** changes short distance $\mathcal{C}_i - \mathcal{C}_i^{SM} = \mathcal{C}_i^{NP}$ and induce new operators, like

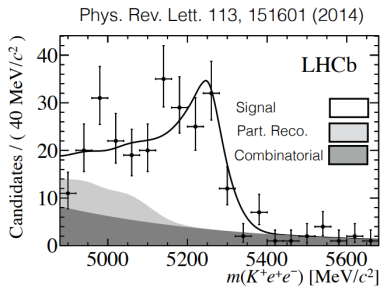
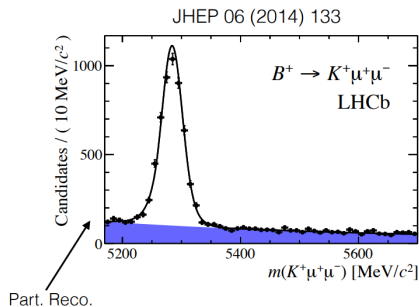
$\mathcal{O}'_{7,9,10} = \mathcal{O}_{7,9,10} (P_L \leftrightarrow P_R) \dots$ also scalars, pseudoscalar, tensor operators...

Anomaly 2

$$R_{K/K^*} = \frac{\mathcal{B}(B \rightarrow K/K^* \mu\mu)}{\mathcal{B}(B \rightarrow K/K^* ee)}$$

Measurement at LHCb

- ⇒ Most precise measurements performed at LHCb.
- ⇒ Main challenge is due to electron Bremsstrahlung.

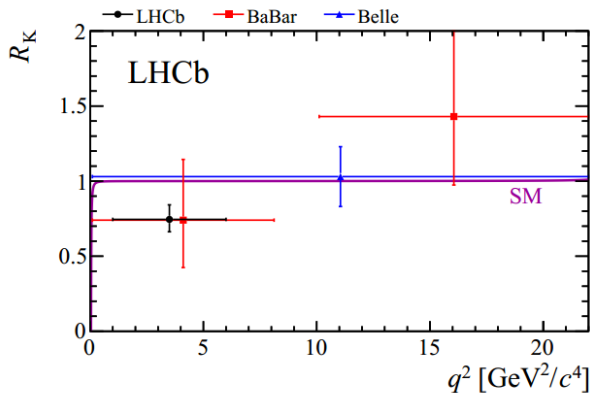


- ⇒ To protect ourselves from electron reconstruction issues we use a double ratio:

$$R_K = \frac{\mathcal{B}(B \rightarrow K \mu \mu) \times \mathcal{B}(B \rightarrow K J/\psi (\rightarrow ee))}{\mathcal{B}(B \rightarrow K ee) \times \mathcal{B}(B \rightarrow K J/\psi (\rightarrow \mu \mu))}$$

Result

$$R_K = 0.745^{+0.090}_{-0.074}(\text{stat.}) \pm 0.036(\text{syst})$$



⇒ 2.6 σ away from SM prediction.

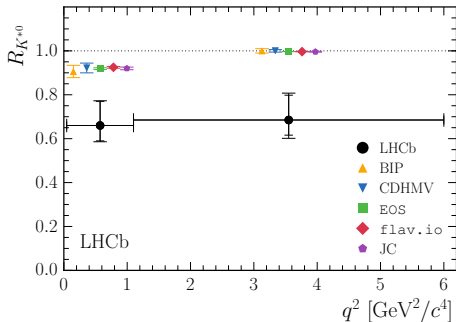
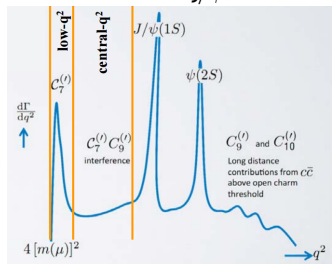
The continuation - R_{K^*}

⇒ The neutral continuation of the R_K measurement is to measure its partner:

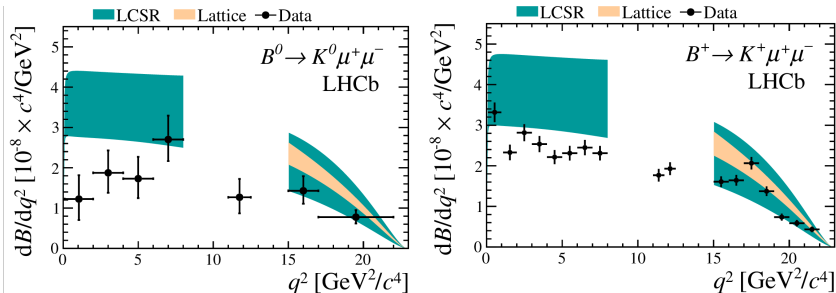
$$R_{K^*} = \frac{\mathcal{B}(B \rightarrow K^* \mu \mu)}{\mathcal{B}(B \rightarrow K^* e e)}$$

⇒ Measurement performed in two q^2 bins.

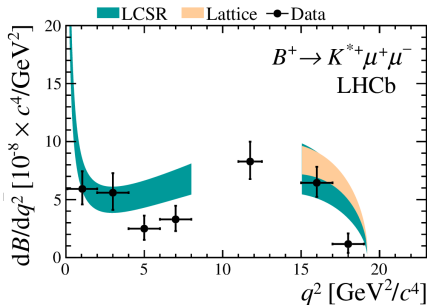
⇒ Normalized in double ratio to $B \rightarrow K^* J/\psi$.



Branching fraction measurements of $B \rightarrow K^{*\pm} \mu \mu$



- Despite large theoretical errors the results are consistently smaller than SM prediction.



Anomaly 3

$$P'_5 = \sqrt{2} \frac{\Re(A_{\perp}^L A_{\parallel}^{L*} - A_{\perp}^R A_{\parallel}^{R*})}{\sqrt{|A_0|^2 (|A_{\perp}|^2 + |A_0|^2)}}$$

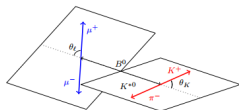
$B^0 \rightarrow K^* \mu^- \mu^+$ kinematics

\Rightarrow The kinematics of $B^0 \rightarrow K^* \mu^- \mu^+$ decay is described by three angles θ_l , θ_k , ϕ and invariant mass of the dimuon system (q^2).

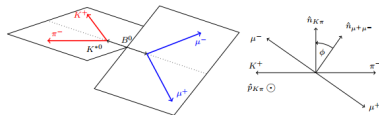
$\Rightarrow \cos \theta_k$: the angle between the direction of the kaon in the K^* ($\overline{K^*}$) rest frame and the direction of the K^* ($\overline{K^*}$) in the B^0 ($\overline{B^0}$) rest frame.

$\Rightarrow \cos \theta_l$: the angle between the direction of the μ^- (μ^+) in the dimuon rest frame and the direction of the dimuon in the B^0 ($\overline{B^0}$) rest frame.

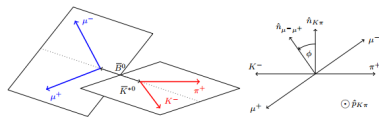
$\Rightarrow \phi$: the angle between the plane containing the μ^- and μ^+ and the plane containing the kaon and pion from the K^* .



(a) θ_k and θ_l definitions for the B^0 decay



(b) ϕ definition for the B^0 decay



(c) ϕ definition for the B^0 decay

$B^0 \rightarrow K^* \mu^- \mu^+$ kinematics

\Rightarrow The kinematics of $B^0 \rightarrow K^* \mu^- \mu^+$ decay is described by three angles θ_l, θ_K, ϕ and invariant mass of the dimuon system (q^2).

$$\frac{d^4\Gamma}{dq^2 d\cos\theta_K d\cos\theta_l d\phi} = \frac{9}{32\pi} \left[J_{1s} \sin^2\theta_K + J_{1c} \cos^2\theta_K + (J_{2s} \sin^2\theta_K + J_{2c} \cos^2\theta_K) \cos 2\theta_l \right. \\ \left. + J_3 \sin^2\theta_K \sin^2\theta_l \cos 2\phi + J_4 \sin 2\theta_K \sin 2\theta_l \cos \phi + J_5 \sin 2\theta_K \sin \theta_l \cos \phi \right. \\ \left. + (J_{6s} \sin^2\theta_K + J_{6c} \cos^2\theta_K) \cos \theta_l + J_7 \sin 2\theta_K \sin \theta_l \sin \phi + J_8 \sin 2\theta_K \sin 2\theta_l \sin \phi \right. \\ \left. + J_9 \sin^2\theta_K \sin^2\theta_l \sin 2\phi \right],$$

\Rightarrow This is the most general expression of this kind of decay.

\Rightarrow The 12 observables (J_i) can be reduced to 8 thanks to some symmetries.

Transversity amplitudes

⇒ One can link the angular observables to transversity amplitudes

$$J_{1s} = \frac{(2 + \beta_\ell^2)}{4} \left[|A_\perp^L|^2 + |A_\parallel^L|^2 + |A_\perp^R|^2 + |A_\parallel^R|^2 \right] + \frac{4m_\ell^2}{q} \operatorname{Re} \left(A_\perp^L A_\perp^{R*} + A_\parallel^L A_\parallel^{R*} \right),$$

$$J_{1c} = |A_0^L|^2 + |A_0^R|^2 + \frac{4m_\ell^2}{q} \left[|A_t|^2 + 2\operatorname{Re}(A_0^L A_0^{R*}) \right] + \beta_\ell^2 |A_S|^2,$$

$$J_{2s} = \frac{\beta_\ell^2}{4} \left[|A_\perp^L|^2 + |A_\parallel^L|^2 + |A_\perp^R|^2 + |A_\parallel^R|^2 \right], \quad J_{2c} = -\beta_\ell^2 \left[|A_0^L|^2 + |A_0^R|^2 \right],$$

$$J_3 = \frac{1}{2} \beta_\ell^2 \left[|A_\perp^L|^2 - |A_\parallel^L|^2 + |A_\perp^R|^2 - |A_\parallel^R|^2 \right], \quad J_4 = \frac{1}{\sqrt{2}} \beta_\ell^2 \left[\operatorname{Re}(A_0^L A_\parallel^{L*} + A_0^R A_\parallel^{R*}) \right],$$

$$J_5 = \sqrt{2} \beta_\ell \left[\operatorname{Re}(A_0^L A_\perp^{L*} - A_0^R A_\perp^{R*}) - \frac{m_\ell}{\sqrt{q^2}} \operatorname{Re}(A_\parallel^L A_S^* + A_\parallel^{R*} A_S) \right],$$

$$J_{6s} = 2\beta_\ell \left[\operatorname{Re}(A_\parallel^L A_\perp^{L*} - A_\parallel^R A_\perp^{R*}) \right], \quad J_{6c} = 4\beta_\ell \frac{m_\ell}{\sqrt{q^2}} \operatorname{Re}(A_0^L A_S^* + A_0^{R*} A_S),$$

$$J_7 = \sqrt{2} \beta_\ell \left[\operatorname{Im}(A_0^L A_\parallel^{L*} - A_0^R A_\parallel^{R*}) + \frac{m_\ell}{\sqrt{q^2}} \operatorname{Im}(A_\perp^L A_S^* - A_\perp^{R*} A_S) \right],$$

$$J_8 = \frac{1}{\sqrt{2}} \beta_\ell^2 \left[\operatorname{Im}(A_0^L A_\perp^{L*} + A_0^R A_\perp^{R*}) \right], \quad J_9 = \beta_\ell^2 \left[\operatorname{Im}(A_\parallel^{L*} A_\perp^L + A_\parallel^{R*} A_\perp^R) \right],$$

Link to effective operators

⇒ So here is where the magic happens. At leading order the amplitudes can be written as:

$$A_{\perp}^{L,R} = \sqrt{2} N m_B (1 - \hat{s}) \left[(C_9^{\text{eff}} + C_9^{\text{eff}'}) \mp (C_{10} + C'_{10}) + \frac{2\hat{m}_b}{\hat{s}} (C_7^{\text{eff}} + C_7^{\text{eff}'}) \right] \xi_{\perp}(E_{K^*})$$

$$A_{\parallel}^{L,R} = -\sqrt{2} N m_B (1 - \hat{s}) \left[(C_9^{\text{eff}} - C_9^{\text{eff}'}) \mp (C_{10} - C'_{10}) + \frac{2\hat{m}_b}{\hat{s}} (C_7^{\text{eff}} - C_7^{\text{eff}'}) \right] \xi_{\perp}(E_{K^*})$$

$$A_0^{L,R} = -\frac{N m_B (1 - \hat{s})^2}{2\hat{m}_{K^*} \sqrt{\hat{s}}} \left[(C_9^{\text{eff}} - C_9^{\text{eff}'}) \mp (C_{10} - C'_{10}) + 2\hat{m}_b (C_7^{\text{eff}} - C_7^{\text{eff}'}) \right] \xi_{\parallel}(E_{K^*}),$$

where $\hat{s} = q^2/m_B^2$, $\hat{m}_i = m_i/m_B$. The $\xi_{\parallel,\perp}$ are the form factors.

Link to effective operators

⇒ So here is where the magic happens. At leading order the amplitudes can be written as:

$$A_{\perp}^{L,R} = \sqrt{2} N m_B (1 - \hat{s}) \left[(C_9^{\text{eff}} + C_9^{\text{eff}'}) \mp (C_{10} + C'_{10}) + \frac{2\hat{m}_b}{\hat{s}} (C_7^{\text{eff}} + C_7^{\text{eff}'}) \right] \xi_{\perp}(E_{K^*})$$

$$A_{\parallel}^{L,R} = -\sqrt{2} N m_B (1 - \hat{s}) \left[(C_9^{\text{eff}} - C_9^{\text{eff}'}) \mp (C_{10} - C'_{10}) + \frac{2\hat{m}_b}{\hat{s}} (C_7^{\text{eff}} - C_7^{\text{eff}'}) \right] \xi_{\perp}(E_{K^*})$$

$$A_0^{L,R} = -\frac{N m_B (1 - \hat{s})^2}{2\hat{m}_{K^*} \sqrt{\hat{s}}} \left[(C_9^{\text{eff}} - C_9^{\text{eff}'}) \mp (C_{10} - C'_{10}) + 2\hat{m}_b (C_7^{\text{eff}} - C_7^{\text{eff}'}) \right] \xi_{\parallel}(E_{K^*}),$$

where $\hat{s} = q^2/m_B^2$, $\hat{m}_i = m_i/m_B$. The $\xi_{\parallel,\perp}$ are the form factors.

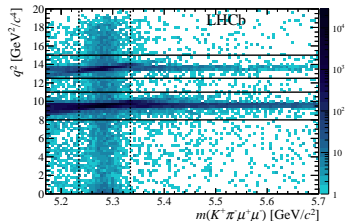
⇒ Now we can construct observables that cancel the ξ form factors at leading order:

$$P'_5 = \frac{J_5 + \bar{J}_5}{2\sqrt{-(J_2^c + \bar{J}_2^c)(J_2^s + \bar{J}_2^s)}}$$

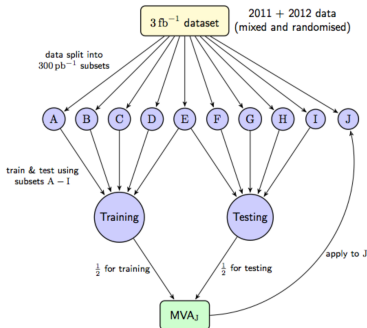
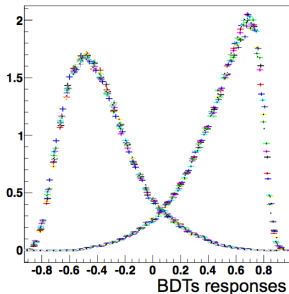
LHCb measurement of $B_d^0 \rightarrow K^* \mu \mu$

Multivariate selection

- PID, kinematics and isolation variables used in a Boosted Decision Tree (BDT) to discriminate signal and background.
- BDT with k-Folding technique.
- Completely data driven.



MVA_baseline_S



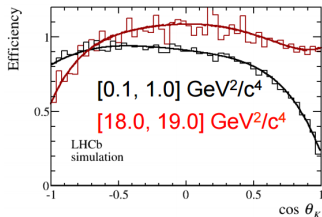
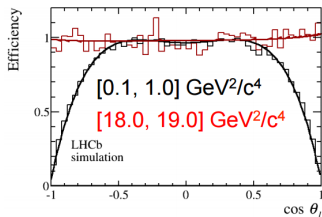
Detector acceptance

- Detector distorts our angular distribution.
- We need to model this effect.
- 4D function is used:

$$\epsilon(\cos \theta_l, \cos \theta_k, \phi, q^2) = \sum_{ijkl} P_i(\cos \theta_l) P_j(\cos \theta_k) P_k(\phi) P_l(q^2),$$

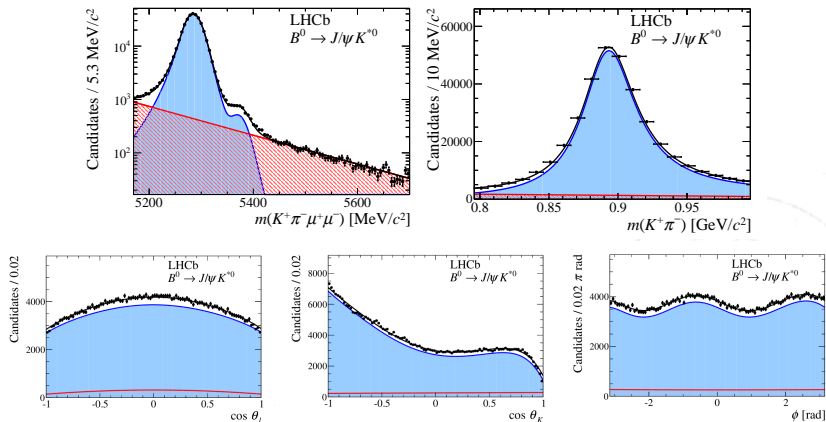
where P_i is the Legendre polynomial of order i .

- We use up to 4th, 5th, 6th, 5th order for the $\cos \theta_l, \cos \theta_k, \phi, q^2$.
- The coefficients were determined using Method of Moments, with a huge simulation sample.
- The simulation was done assuming a flat phase space and reweighting the q^2 distribution to make it flat.
- To make this work the q^2 distribution needs to be reweighted to be flat.



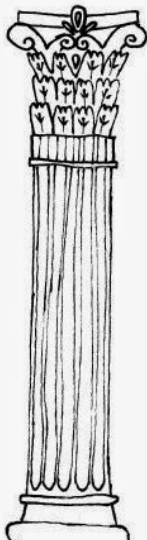
Control channel

- We tested our unfolding procedure on $B \rightarrow J/\psi K^*$.
- The result is in perfect agreement with other experiments and our different analysis of this decay.

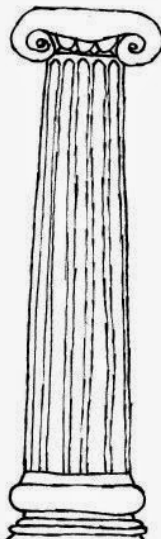


The columns of New Physics

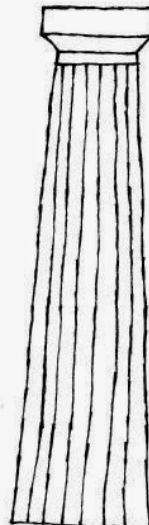
Amplitudes



Maximum likelihood fit



Method of Moments



The columns of New Physics

1. Maximum likelihood fit:

- The most standard way of obtaining the parameters.
- Suffers from convergence problems, under coverages, etc. in low statistics.

2. Method of moments:

- Less precise than the likelihood estimator (10 – 15% larger uncertainties).
- Does not suffer from the problems of likelihood fit.

3. Amplitude fit:

- Incorporates all the physical symmetries inside the amplitudes! The most precise estimator.
- Has theoretical assumptions inside!

Maximum likelihood fit - Results

⇒ In the maximum likelihood fit one could weight the events accordingly to the $\frac{1}{\epsilon(\cos \theta_l, \cos \theta_k, \phi, q^2)}$

⇒ Better alternative is to put the efficiency into the maximum likelihood fit itself:

⇒ Better alternative is to put the efficiency into the maximum likelihood fit itself:

$$\mathcal{L} = \prod_{i=1}^N \epsilon_i(\Omega_i, q_i^2) \mathcal{P}(\Omega_i, q_i^2) / \int \epsilon(\Omega, q^2) \mathcal{P}(\Omega, q^2) d\Omega dq^2$$

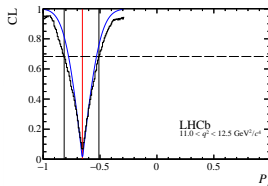
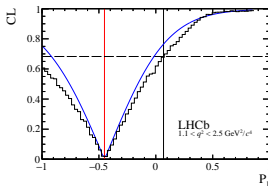
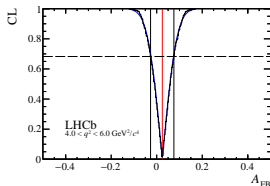
⇒ Only the relative weights matters!

⇒ The Procedure was commissioned with TOY MC study.

⇒ Use Feldmann-Cousins to determine the uncertainties.

⇒ Angular background component is modelled with 2nd order Chebyshev polynomials, which was tested on the side-bands.

⇒ S-wave component treated as nuisance parameter.



Method of moments

⇒ See [Phys.Rev.D91\(2015\)114012](#), F.Beaujean , M.Chrzaszcz, N.Serra, D. van Dyk for details.

⇒ The idea behind Method of Moments is simple: Use orthogonality of spherical harmonics, $f_j(\vec{\Omega})$ to solve for coefficients within a q^2 bin:

$$\int f_i(\vec{\Omega})f_j(\vec{\Omega}) = \delta_{ij}$$

$$M_i = \int \left(\frac{1}{d(\Gamma + \bar{\Gamma})/dq^2} \right) \frac{d^3(\Gamma + \bar{\Gamma})}{d\vec{\Omega}} f_i(\vec{\Omega}) d\Omega$$

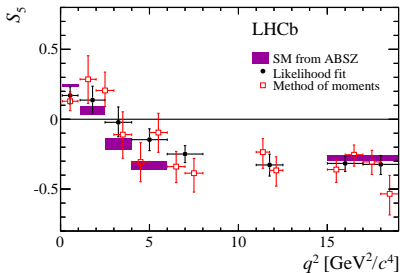
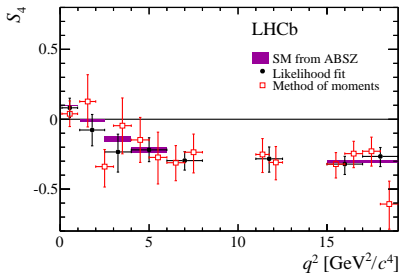
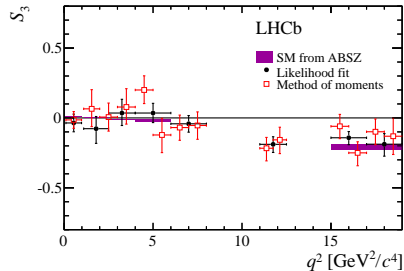
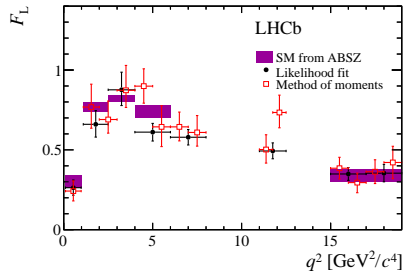
⇒ Don't have true angular distribution but we "sample" it with our data.

⇒ Therefore: $\int \rightarrow \sum$ and $M_i \rightarrow \hat{M}_i$

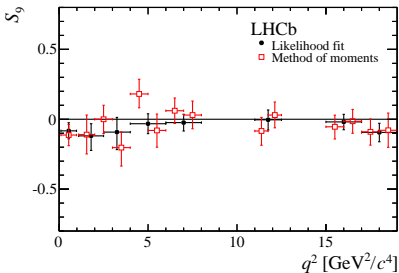
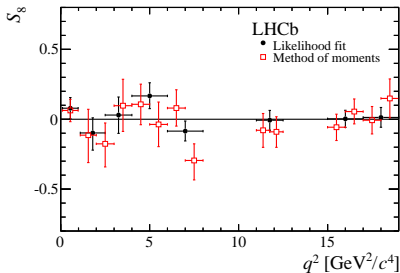
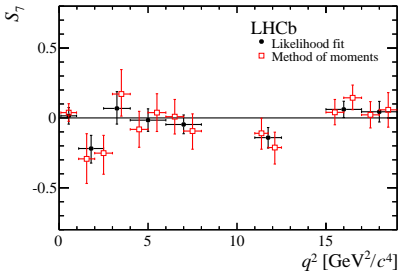
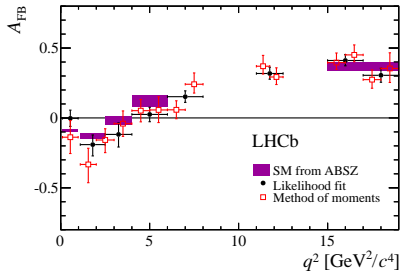
$$\hat{M}_i = \frac{1}{\sum_e \omega_e} \sum_e \omega_e f_i(\vec{\Omega}_e)$$

⇒ The weight ω accounts for the efficiency. Again the normalization of weights does not matter.

Method of moments - results

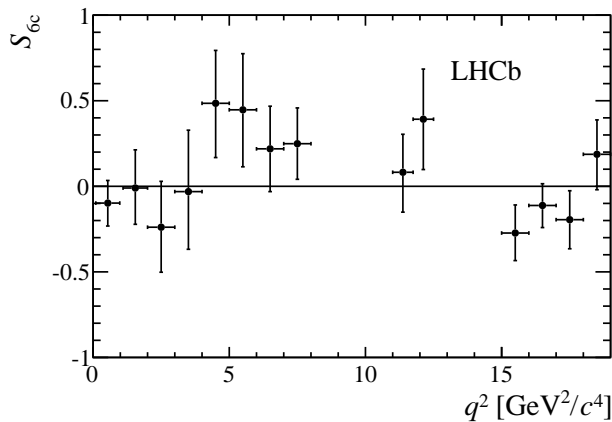


Method of moments - results



Method of moments - results

⇒ Method of Moments allowed us to measure for the first time a new observable:



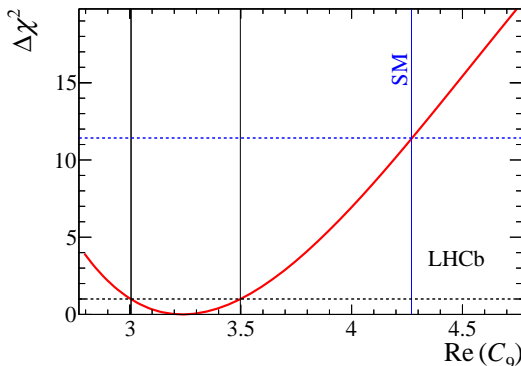
Compatibility with SM

- ⇒ Use EOS software package to test compatibility with SM.
- ⇒ Perform the χ^2 fit to the measured:

$$F_L, A_{FB}, S_{3,\dots,9}.$$

- ⇒ Float a vector coupling: $\Re(C_9)$.
- ⇒ Best fit is found to be 3.4σ away from the SM.

$$\Delta\mathfrak{R}(C_9) \equiv \mathfrak{R}(C_9)^{\text{fit}} - \mathfrak{R}(C_9)^{\text{SM}} = -1.03$$



Global picture of P_5'

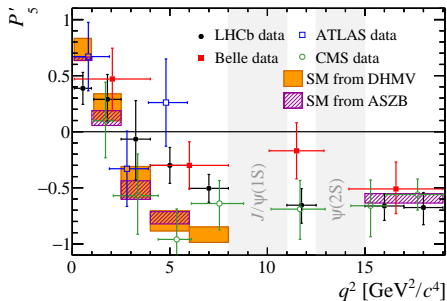
⇒ 2013 LHCb:
arXiv::1308.1707

⇒ 2015 LHCb:
arXiv::1512.0444

⇒ 2016 Belle:
arXiv::1604.04042

⇒ 2017:
ATLAS-CONF-2017-023
(20.5 fb^{-1}) and
CMS-PAS-BPH-15-008
(20.8 fb^{-1})

⇒ Theory: DHMV: arXiv::1407.8526
ASZB: arXiv::1411.3161



Global fit to $b \rightarrow sll$ measurements

Link the observables

⇒ Fits prepare by S. Descotes-Genon, L. Hofer, J. Matias, J. Virto, [arXiv::1510.04239](https://arxiv.org/abs/1510.04239)

- Inclusive

- $B \rightarrow X_s \gamma$ (BR) $c_7^{(\prime)}$
- $B \rightarrow X_s \ell^+ \ell^-$ (dBR/dq^2) $c_7^{(\prime)}, c_9^{(\prime)}, c_{10}^{(\prime)}$

- Exclusive leptonic

- $B_s \rightarrow \ell^+ \ell^-$ (BR) $c_{10}^{(\prime)}$

- Exclusive radiative/semileptonic

- $B \rightarrow K^* \gamma$ (BR, S, A_T) $c_7^{(\prime)}$
- $B \rightarrow K \ell^+ \ell^-$ (dBR/dq^2) $c_7^{(\prime)}, c_9^{(\prime)}, c_{10}^{(\prime)}$
- **$B \rightarrow K^* \ell^+ \ell^-$** (dBR/dq^2 , **Optimized Angular Obs.**) .. $c_7^{(\prime)}, c_9^{(\prime)}, c_{10}^{(\prime)}$
- $B_s \rightarrow \phi \ell^+ \ell^-$ (dBR/dq^2 , Angular Observables) $c_7^{(\prime)}, c_9^{(\prime)}, c_{10}^{(\prime)}$
- $\Lambda_b \rightarrow \Lambda \ell^+ \ell^-$ (None so far)
- etc.

Statistic details

⇒ Frequentist approach:

$$\chi^2(C_i) = [O_{\text{exp}} - O_{\text{th}}(C_i)]_j [Cov^{-1}]_{jk} [O_{\text{exp}} - O_{\text{th}}(C_i)]_k$$

- $\mathbf{Cov} = \mathbf{Cov}^{\text{exp}} + \mathbf{Cov}^{\text{th}}$. We have Cov^{exp} for the first time
- Calculate Cov^{th} : correlated multigaussian scan over all nuisance parameters
- Cov^{th} depends on C_i : Must check this dependence

For the Fit:

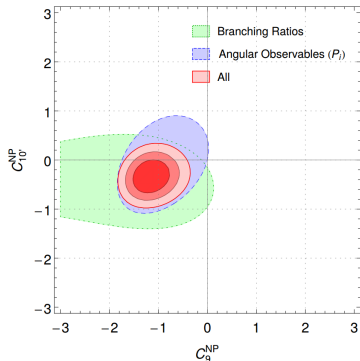
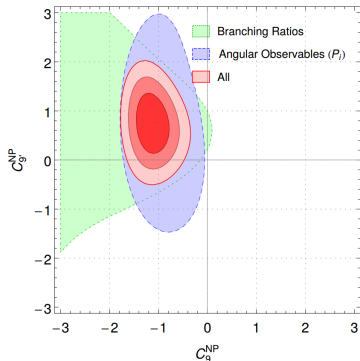
- Minimise $\chi^2 \rightarrow \chi_{\text{min}}^2 = \chi^2(C_i^0)$ (Best Fit Point = C_i^0)
- Confidence level regions: $\chi^2(C_i) - \chi_{\text{min}}^2 < \Delta\chi_{\sigma,n}$

⇒ The results from 1D scans:

Coefficient $C_i^{\text{NP}} = C_i - C_i^{\text{SM}}$	Best fit	1σ	3σ	Pull_{SM}
C_9^{NP}	-1.09	[-1.29, -0.87]	[-1.67, -0.39]	4.5 ←
$C_9^{\text{NP}} = -C_{10}^{\text{NP}}$	-0.68	[-0.85, -0.50]	[-1.22, -0.18]	4.2 ←
$C_9^{\text{NP}} = -C_{9'}^{\text{NP}}$	-1.06	[-1.25, -0.86]	[-1.60, -0.40]	4.8 ← (no R_F)

Theory implications

- The data can be explained by modifying the C_9 Wilson coefficient.
- Overall there is around 4.5σ discrepancy wrt. SM.

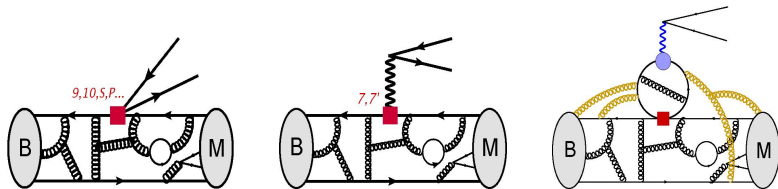


2D scans

Coefficient	Best Fit Point	Pull _{SM}
$(\mathcal{C}_7^{\text{NP}}, \mathcal{C}_9^{\text{NP}})$	$(-0.00, -1.07)$	4.1
$(\mathcal{C}_9^{\text{NP}}, \mathcal{C}_{10}^{\text{NP}})$	$(-1.08, 0.33)$	4.3
$(\mathcal{C}_9^{\text{NP}}, \mathcal{C}_{7'}^{\text{NP}})$	$(-1.09, 0.02)$	4.2
$(\mathcal{C}_9^{\text{NP}}, \mathcal{C}_{9'}^{\text{NP}})$	$(-1.12, 0.77)$	4.5
$(\mathcal{C}_9^{\text{NP}}, \mathcal{C}_{10'}^{\text{NP}})$	$(-1.17, -0.35)$	4.5
$(\mathcal{C}_9^{\text{NP}} = -\mathcal{C}_{9'}^{\text{NP}}, \mathcal{C}_{10}^{\text{NP}} = \mathcal{C}_{10'}^{\text{NP}})$	$(-1.15, 0.34)$	4.7
$(\mathcal{C}_9^{\text{NP}} = -\mathcal{C}_{9'}^{\text{NP}}, \mathcal{C}_{10}^{\text{NP}} = -\mathcal{C}_{10'}^{\text{NP}})$	$(-1.06, 0.06)$	4.4
$(\mathcal{C}_9^{\text{NP}} = \mathcal{C}_{9'}^{\text{NP}}, \mathcal{C}_{10}^{\text{NP}} = \mathcal{C}_{10'}^{\text{NP}})$	$(-0.64, -0.21)$	3.9
$(\mathcal{C}_9^{\text{NP}} = -\mathcal{C}_{10}^{\text{NP}}, \mathcal{C}_{9'}^{\text{NP}} = \mathcal{C}_{10'}^{\text{NP}})$	$(-0.72, 0.29)$	3.8

- $\mathcal{C}_9^{\text{NP}}$ always play a dominant role
- All 2D scenarios above 4σ are quite indistinguishable.

$B \rightarrow K^* \ell \ell$ Amplitudes



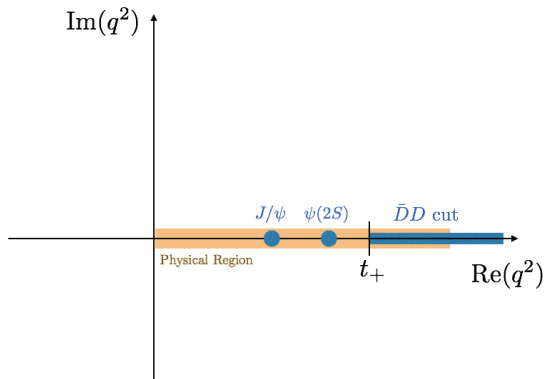
$$A_{\lambda}^{L,R} = N_{\lambda} \left\{ (C_9 \mp C_{10}) \mathcal{F}_{\lambda}(q^2) + \frac{2m_b M_B}{q^2} \left[C_7 \mathcal{F}_{\lambda}^T(q^2) - 16\pi^2 \frac{M_B}{m_b} \mathcal{H}_{\lambda}(q^2) \right] \right\}$$

- ▶ Local (Form Factors) : $\mathcal{F}_{\lambda}^{(T)}(q^2) = \langle \bar{M}_{\lambda}(k) | \bar{s} \Gamma_{\lambda}^{(T)} b | \bar{B}(k+q) \rangle$
- ▶ Non-Local : $\mathcal{H}_{\lambda}(q^2) = i \mathcal{P}_{\mu}^{\lambda} \int d^4x e^{iq \cdot x} \langle \bar{M}_{\lambda}(k) | T \{ \mathcal{J}_{\text{em}}^{\mu}(x), \mathcal{C}_i \mathcal{O}(0) \} | \bar{B}(q+k) \rangle$
- ▶ CKM structure : $\mathcal{H}_{\lambda} = -\frac{\lambda_u}{\lambda_t} \mathcal{H}_{\lambda}^{(u)} - \frac{\lambda_c}{\lambda_t} \mathcal{H}_{\lambda}^{(c)} \Rightarrow \mathcal{O} \sim (\bar{c}b)(\bar{s}c)$

Analytic structure of $\mathcal{H}_\lambda(q^2)$

[Bobeth, Chrzaszcz, van Dyk, Virto 1707.07305]

Neglecting OZI- and CKM-suppressed contributions :

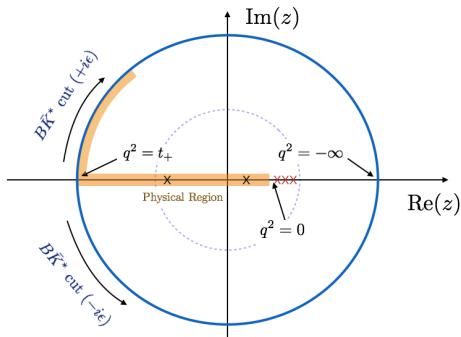
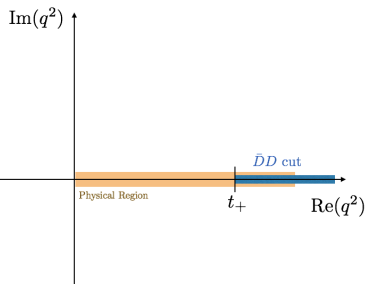


$$\hat{\mathcal{H}}_\lambda(q^2) = (q^2 - M_{J/\psi}^2)(q^2 - M_{\psi(2S)}^2) \mathcal{H}_\lambda(q^2) \quad \text{has no poles.}$$

Accessing $q^2 > 0$: z expansion

[Bobeth, Chrzaszcz, van Dyk, Virto 1707.07305]

► Conformal mapping : $q^2 \mapsto z(q^2) = \frac{\sqrt{t_+ - q^2} - \sqrt{t_+ - t_0}}{\sqrt{t_+ - q^2} + \sqrt{t_+ - t_0}}$



- $\hat{\mathcal{H}}_\lambda(q^2(z))$ is analytic in $|z| < 1$
- Taylor expand $\hat{\mathcal{H}}_\lambda(z)$ around $z = 0$.
- Expansion needed for $|z| < 0.52$ ($-7 \text{ GeV}^2 \leq q^2 \leq 14 \text{ GeV}^2$)

Accessing $q^2 > 0$: z expansion

[Bobeth, Chrzaszcz, van Dyk, Virto 1707.07305]

Some details for actual parametrisation :

- ▶ Try to capture most features of the expansion (better convergence)
- ▶ Parametrize the ratios $\mathcal{H}_\lambda(q^2)/\mathcal{F}_\lambda(q^2)$ instead
- ▶ The poles should not modify the asymptotic behaviour at $|q^2| \rightarrow \infty$

$$\mathcal{H}_\lambda(z) = \frac{1 - z z_{J/\psi}^*}{z - z_{J/\psi}} \frac{1 - z z_{\psi(2S)}^*}{z - z_{\psi(2S)}} \hat{\mathcal{H}}_\lambda(z)$$

$$\hat{\mathcal{H}}_\lambda(z) = \left[\sum_{k=0}^K \alpha_k^{(\lambda)} z^k \right] \mathcal{F}_\lambda(z)$$

where $\alpha_k^{(\lambda)}$ are complex coefficients, and the expansion is truncated after the term z^K . We will take $K = 2$ (16 real parameters).

Experimental constraints on z parametrisation

[Bobeth, Chrzaszcz, van Dyk, Virto 1707.07305]

Experimental constraints :

- ▶ The residues of the poles are given by $B \rightarrow K^* \psi_n$:

$$\mathcal{H}_\lambda(q^2 \rightarrow M_{\psi_n}^2) \sim \frac{M_{\psi_n} f_{\psi_n}^* \mathcal{A}_\lambda^{\psi_n}}{M_B^2 (q^2 - M_{\psi_n}^2)} + \dots$$

- ▶ Angular analyses [Belle, Babar, LHCb] determine :

$$|r_\perp^{\psi_n}|, |r_\parallel^{\psi_n}|, |r_0^{\psi_n}|, \arg\{r_\perp^{\psi_n} r_0^{\psi_n*}\}, \arg\{r_\parallel^{\psi_n} r_0^{\psi_n*}\},$$

where $r_\lambda^{\psi_n} \equiv \text{Res}_{q^2 \rightarrow M_{\psi_n}^2} \frac{\mathcal{H}_\lambda(q^2)}{\mathcal{F}_\lambda(q^2)} \sim \frac{M_{\psi_n} f_{\psi_n}^* \mathcal{A}_\lambda^{\psi_n}}{M_B^2 \mathcal{F}_\lambda(M_{\psi_n}^2)}$

- ▶ We produce correlated pseudo-observables from a fit (5+5).

Prior Fit to \simeq parametrisation

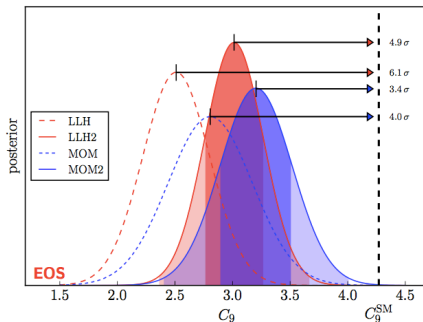
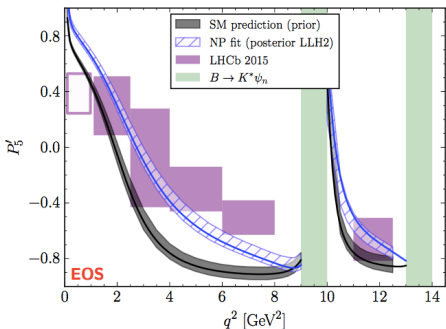
(Prior) Fit to Experimental and theoretical pseudo-observables :

k	0	1	2
$\text{Re}[\alpha_k^{(\perp)}]$	-0.06 ± 0.21	-6.77 ± 0.27	18.96 ± 0.59
$\text{Re}[\alpha_k^{(\parallel)}]$	-0.35 ± 0.62	-3.13 ± 0.41	12.20 ± 1.34
$\text{Re}[\alpha_k^{(0)}]$	0.05 ± 1.52	17.26 ± 1.64	–
$\text{Im}[\alpha_k^{(\perp)}]$	-0.21 ± 2.25	1.17 ± 3.58	-0.08 ± 2.24
$\text{Im}[\alpha_k^{(\parallel)}]$	-0.04 ± 3.67	-2.14 ± 2.46	6.03 ± 2.50
$\text{Im}[\alpha_k^{(0)}]$	-0.05 ± 4.99	4.29 ± 3.14	–

Table: Mean values and standard deviations (in units of 10^{-4}) of the prior PDF for the parameters $\alpha_k^{(\lambda)}$.

New Physics Analysis

SM predictions and Fit including $B \rightarrow K^* \mu^+ \mu^-$ data and C_9^{NP} :



The NP hypothesis with $C_9^{\text{NP}} \sim -1$ is favored strongly in the global fit

Conclusions

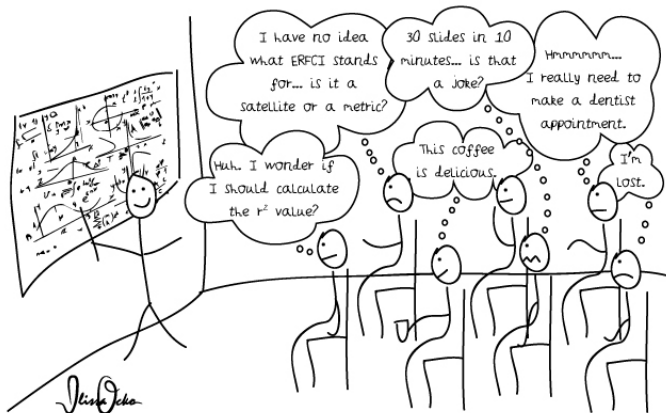
- Clear tensions wrt. SM predictions!
- Measurements cluster in the same direction.
- We are not opening the champagne yet!
- Still need improvement both on theory and experimental side.
- Time will tell if this is QCD+fluctuations or new Physics:

Conclusions

- Clear tensions wrt. SM predictions!
- Measurements cluster in the same direction.
- We are not opening the champagne yet!
- Still need improvement both on theory and experimental side.
- Time will tell if this is QCD+fluctuations or new Physics:

“... when you have eliminated all the Standard Model explanations, whatever remains, however improbable, must be New Physics.”
prof. Joaquim Matias

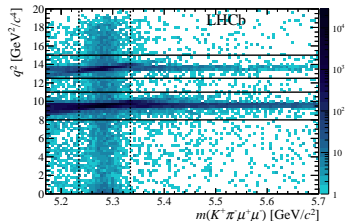
Thank you for the attention!



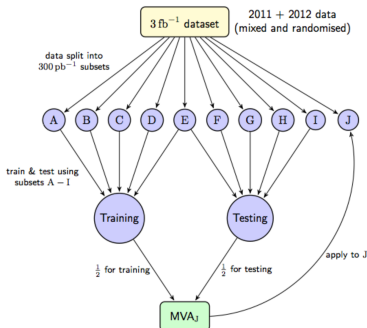
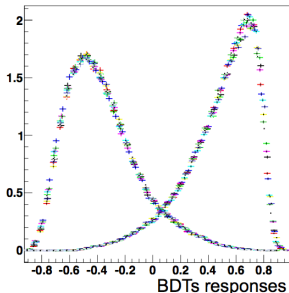
Backup

Multivariate selection

- PID, kinematics and isolation variables used in a Boosted Decision Tree (BDT) to discriminate signal and background.
- BDT with k-Folding technique.
- Completely data driven.

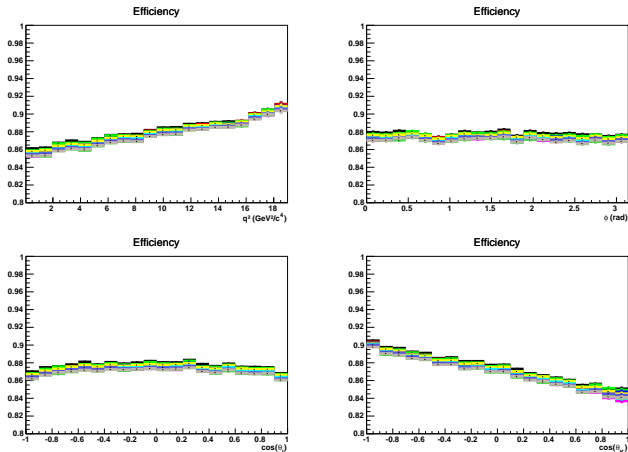


MVA_baseline_S



Multivariate selection, efficiency

⇒ BDT was also checked in order not to bias our angular distribution:



⇒ The BDT has small impact on our angular observables. We will correct for these effects later on.

Amplitudes method

⇒ Fit for amplitudes as (continuous) functions of q^2 in the region: $q^2 \in [1.1.6.0] \text{ GeV}^2/c^4$.

⇒ Needs some Ansatz:

$$A(q^2) = \alpha + \beta q^2 + \frac{\gamma}{q}$$

⇒ The assumption is tested extensively with toys.

⇒ Set of 3 complex parameters α, β, γ per vector amplitude:

- $L, R, 0, \parallel, \perp, \Re, \Im \mapsto 3 \times 2 \times 3 \times 2 = 36$ DoF.
- Scalar amplitudes: +4 DoF.
- Symmetries of the amplitudes reduces the total budget to: 28.

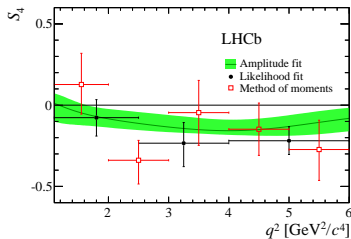
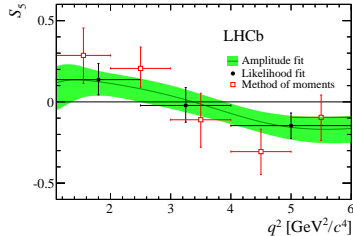
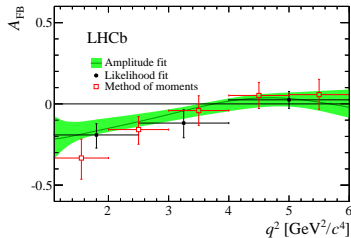
⇒ The technique is described in [JHEP06\(2015\)084](#).

⇒ Allows to build the observables as continuous functions of q^2 :

- At current point the method is limited by statistics.
- In the future the power of this method will increase.

⇒ Allows to measure the zero-crossing points for free and with smaller errors than previous methods.

Amplitudes - results



Zero crossing points:

$$q_0(S_4) < 2.65 \quad \text{at } 95\% \text{ CL}$$

$$q_0(S_5) \in [2.49, 3.95] \quad \text{at } 68\% \text{ CL}$$

$$q_0(A_{FB}) \in [3.40, 4.87] \quad \text{at } 68\% \text{ CL}$$